Properties of dimethacrylate copolymers of varying crosslink density

G. P. Simon
Department of Materials Engineering, Monash University, Clayton, Victoria, Australia 3168

and P. E. M. Allen* and D. R. G. Williams†
*Departments of *Physical and Inorganic Chemistry and †Chemical Engineering, University of Adelaide, GPO Box 498, Adelaide, South Australia 5000*
(Received 29 June 1990; accepted 20 August 1990)

Homopolymers and copolymers of tetrafunctional oligo-ethylene dimethacrylate monomers of widely varying chain lengths are investigated by thermal and fracture techniques. Differential scanning calorimetry of catalysed monomer shows that the polymerization process is inhomogeneous. Quantitative analysis of these results suggest that the mechanism of cure is complex and may be ascribed to complex copolymerization, partial phase separation or a form of interpenetrating network. Dynamic mechanical spectra of the copolymers reveals that their mechanical properties vary monotonically between those of the constituent homopolymers. In some systems, double-peak behaviour is noted in the glass transition region. This is ascribed to possible phase separation. Short rod fracture, a fracture toughness technique suitable for glassy polymers, is also used on a copolymer system to obtain information about the copolymer morphology. The transition from 'stick-slip' to a smoother fracture mode with higher concentrations of the longer, flexible monomer is accompanied by a concomitant decrease in fracture toughness. This behaviour is explained in terms of the inhomogeneity of both homo- and copolymer dimethacrylate systems and failure occurring through points of weakness in the system, the regions of lower crosslink density.

(Keywords: dimethacrylate copolymers; crosslink density; fracture)

INTRODUCTION

Dimethacrylate crosslinked polymers have shown themselves to be of commercial significance in two main fields in recent years, as polymers used in the opto-electronics industry[1,2] and as restorative biomaterials in dentistry[3,4].

The dimethacrylate monomer is tetrafunctional and the reaction mechanism is radical addition polymerization which can be initiated by either heat or ultraviolet (u.v.) light (depending on initiator). The ease of mould filling or coating by the monomer allied with resultant polymer properties (high glass transition temperature, T_g, hardness and excellent dimensional and thermal stability) make these systems very useful as replication materials in the production of laser video discs[1,5], optical fibre claddings[6] and aspherical lenses[7]. In dentistry, inorganic fillers and glasses are introduced into these network polymers to improve wear resistance[8,9]. To minimize the level of fillers and thus produce a restorative material of pleasant appearance, highly crosslinked polymers are generally required. However, too high a crosslink density results in a very brittle structure. With such a wide range of applications and material properties demanded of crosslinked systems it is important to be able to tailor polymer properties to suit their end use requirements. One such method of modification is copolymerization.

The dimethacrylate homologues investigated in this work have the chemical structure:

$$H_2C{=}C(CH_3).CO{\cdot}O{\cdot}(CH_2CH_2O)_n{\cdot}CO{\cdot}C(CH_3){=}CH_2$$

A range of monomers with oligo-ethylene (OE) chain length varying from $n=1$ to 4 and $n=9$ to 22 are readily commercially available and as they are often collectively labelled as oligoester acrylate systems they will be denoted by the acronym OEA in this paper[11]. The resultant homopolymers' physical state at room temperature ranges from a glass for $n \leqslant 4$ to rubbery for $n>9$. Altering the length of the OE unit (and thus network crosslink density) has a number of effects on the properties of the polymerization reaction and resultant homopolymer properties. Increasing the OE length causes the monomer unit to become more flexible resulting in faster rates of polymerization and higher attainable levels of reaction[10,11]. The basic nature of the dimethacrylate reaction is found to be inhomogeneous[12–14] with a 'porridge-like' structure, involving micro-regions of high crosslink density surrounded by regions of lower crosslink density. The resultant morphology is a function of OE length.

Some work has been published on copolymer systems of diallyl phthalate with various length ethylene glycol bis(allyl phthalate) monomers[16]. In addition interpenetrating networks of thermal and u.v. cured tetrafunctional, crosslinked systems[15] have been investigated. However, no work has been reported (to our knowledge) on copolymers of the dimethacrylate series despite their technological and academic importance and interest.

We concentrate in this work on copolymerization of dimethacrylate monomers of vastly different OE length. Such monomers, homopolymerized, result in polymers of greatly contrasting mechanical properties. The effect of the OE chain length on homopolymer properties is initially examined, followed by an investigation of copolymerization between dimethacrylates with $n=13$

0032-3861/91/142577-11

and monomers of length $n=2$, 3 and 4, respectively. This allows us to monitor the effect of increasing OE length on copolymer properties.

EXPERIMENTAL

Poly(ethylene glycol) dimethacrylates with values of $n=2$, 3 and 4 were obtained from Fluka whilst $n=13$ was obtained from Polyscience. The monomers (and by implication the homopolymers that result) will be referred to in this paper as PEGDM(n). The liquid monomers were dried and stored over molecular sieves. It was found[17] that removal of inhibitor does not affect the mechanical properties and there was no attempt made to remove it from the monomer. The initiator used was tert-butyl-2-ethyl peroxyhexanoate, obtained from Interrox, Australia. Prior to any polymerization the monomer had high purity nitrogen gas bubbled through it for ~20 min to remove dissolved oxygen which may inhibit the radical reaction.

The thermal characteristics of the curing reaction of both the catalysed homo- and comonomers were investigated by differential scanning calorimetry (d.s.c.) of catalysed monomer, sealed under nitrogen in aluminium sample pans. A Perkin Elmer DSC was used with a scanning rate of 10°C min^{-1}. By observing in some detail the curing behaviour of homo- and comonomers, inferences are drawn in this work about the final polymer structure.

The polymers and copolymers produced were subjected to two main mechanical tests—dynamic mechanical analysis (torsion pendulum) and fracture toughness (short rod fracture).

The samples for dynamic mechanical analysis were cast using the technique described by Cowperthwaite *et al.*[18] in which silicone tubing is used as an air-tight spacer between sheets of glass. Into this mould oxygen-free, catalysed monomer is poured and cured in an oven. The torsion pendulum used was built in this laboratory to cover a temperature range −150 to 200°C. It is a counterbalanced, rotational system in which the sample is pulsed by means of an electromagnet which delivers a predetermined torque pulse to the device's inertial arms and the natural decay of the sample's oscillation was measured. The parameters determined are shear storage modulus, G', loss shear modulus, G'', and the loss tangent, $\tan\delta$. The average measuring frequency is ~1 Hz. Sample size was $\sim 1.5\times 9\times 30$ mm. Sample temperature was maintained by circulating high purity, dry nitrogen throughout the measurement chamber. This has the added advantage of preventing moisture deposition on the samples during measurement at sub-zero temperatures.

The polymer fracture toughness in this work is quantified by determining K_{IC}, the critical stress intensity for the initiation of cracks. The greater the energy dissipative fracture mechanisms in a system, the greater the value of K_{IC}. Conventional methods of measuring fracture toughness such as the notched, three-point method are often inappropriate for crosslinked systems due to brittle failure and rapid crack growth in these materials.

A technique has been developed by Barker[19,20] which encourages stable crack growth in thermosetting systems whilst employing small samples and maintaining the plane–strain conditions necessary for valid K_{IC} measurement[21]. It is known as the short rod fracture toughness technique.

The geometry of the sample is shown in *Figure 1*. It consists of a small rod-shaped sample with a chevron slit and side notches. In the experiment a wedge is placed in the mouth of the slot and a load applied whilst the mouth opening displacement is measured as a function of the load. The crack initiates at the tip of the notch and, because it then propagates along an increasingly wider crack front, becomes stable. It is found that when the crack reaches a critical length, a_c (which is geometry, not material, dependent) a maximum load occurs, related to K_{IC} (MN $m^{-3/2}$) by the equation

$$K_{IC}=A\times P_c\times B^{0.5} \tag{1}$$

where B=rod diameter, P_c=peak load at a_c and A=calibration constant. Provided that a prescribed geometry (relative dimensions of the sample) is adhered to, the calibration constant is dimensionless and independent of absolute size of the test piece. For the geometry[20] shown in *Figure 1* it has the value 20.8.

Although K_{IC} is, by definition, related to crack initiation, it has been shown by Barker[20] that K_{IC} in this experiment is related more closely to steady state crack propagation. Further, Barker[20] demonstrates that there is good correlation between results from this technique and other fracture toughness measurements because most other plane–strain K_{IC}-determining techniques also involve measurement of steady state crack properties[22].

Fracture samples of PEGDM(4) and PEGDM(13) were made by the polymerization of catalysed monomer in appropriately shaped Teflon moulds. The notch tip was prenotched with a razor blade to guide the crack. The grips were of a cylindrical crown shape[23] to maintain axial loading and are driven by an Instron testing device. The strain transducer was attached directly to the specimen mouth and fed back into the Instron. All tests were performed at room temperature and a low crosshead speed of 1 mm min^{-1} was used to promote stable crack growth.

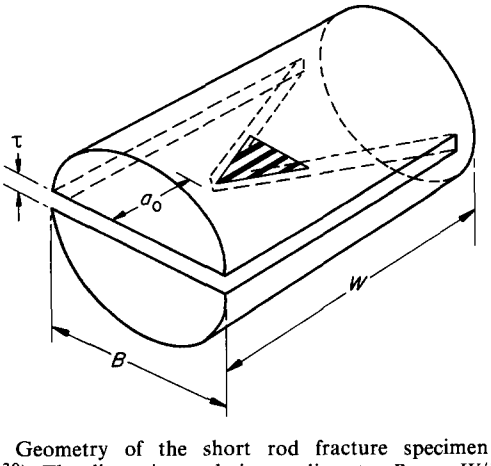

Figure 1 Geometry of the short rod fracture specimen (after Barker[19,20]). The dimensions relative to diameter B are: $W/B=1.5$, $\tau/B=0.03$, $a_0/B=0.53$ and angle of slot = 55.2°

RESULTS AND DISCUSSION

The d.s.c. curves of initiated neat monomer PEGDM(2), PEGDM(3), PEGDM(4) and PEGDM(13) are shown in *Figure 2*. The thermograms are exothermic and presented qualitatively for comparison. Quantifiable parameters from these curves such as the temperature of peak maxima, T_p, the peak broadness (width at half height) and the total heat of the polymerization reaction, ΔH_{cure} (area under exotherm in kJ mol^{-1}) are presented in *Table 1*.

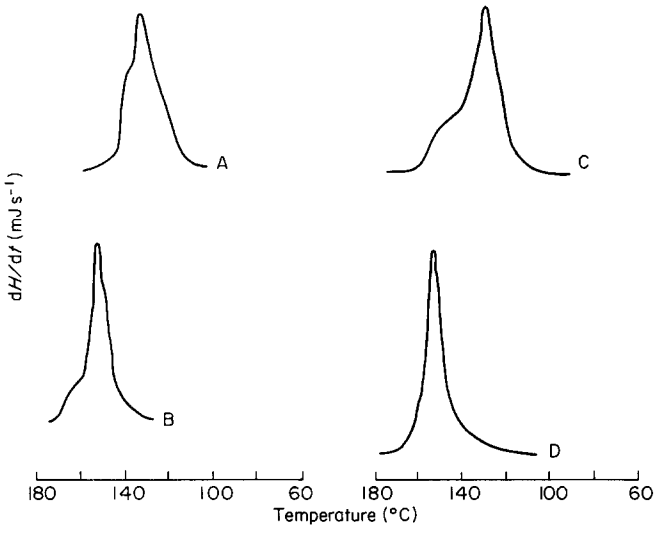

Figure 2 Typical d.s.c. polymerization exotherms produced by the thermal scanning of neat OEA monomers catalysed with 0.2% initiator. The monomers are: (A) PEGDM(2); (B) PEGDM(3); (C) PEGDM(4); (D) PEGDM(13). The scan rate is 10°C min^{-1}

Figure 2 shows that all the pure monomers scanned [except PEGDM(13)] show high temperature shoulders. The temperature location of the shoulders for each system is: PEGDM(2), 137°C; PEGDM(3), 155°C; and PEGDM(4), 155°C. Without a specific mathematical model to allow curve-fitting of the thermograms it is difficult to deconvolute what appears to be largely a two-stage process. A rough hand-fit indicates that the area under the high temperature shoulder is 15–20% of the total exothermic energy.

The high temperature shoulder in this temperature scanning experiment of the three shortest OE chain length monomers is indicative of at least a two-stage curing process for the homopolymers. Both Moore[24] and Horie[28] found dual exotherm peaks in dimethacrylate systems in isothermal experiments and ascribed this behaviour to autoacceleration. This process involves a decrease in the radical termination rate constant due to increased viscosity of the reacting medium. Because the polymer propagation rate continues relatively unchanged the result is an increase in the overall rate of the polymerization reaction. In highly crosslinked tetrafunctional systems autoacceleration is likely to occur at very low levels of cure since viscosity increases significantly at a very early stage in the reaction. However, this effect usually occurs at $<10\%$ cure in these systems[17] whereas the high temperature shoulder on the OEA exotherms occurs at $\sim 80\%$ cure. An explanation for the shoulder is that the main peak is energy liberated by the bulk, inhomogeneous polymerization reaction and the high temperature shoulder is the curing of the low molecular weight unsaturation (monomer and chain ends) that resides between the highly crosslinked regions. Since this latter reaction occurs subsequent to the main, inhomogeneous polymerization of highly crosslinked nodules,

Table 1 Differential scanning calorimetric results from thermal scanning of catalysed OEA homo- and copolymer systems

Mass % PEGDM(13)	Mol % PEGDM(13)	Peak A (°C)[a]	Peak B (°C)[a]	ΔH (kJ mol^{-1}) (experimental)	ΔH (kJ mol^{-1}) (weighted)
Copolymers of PEGDM(13) and PEGDM(2)					
0	0	133 4(12)	–	115.2± 6.1	115.2
53	27	141 3(11)	167 2(12)	133.6±14.1	107.3
74	49	149 2(14)	187 1(14)	141.3±10.1	100.9
89	72	142 2(8)	180 5(12)	139.6±11.2	94.7
100	100	144 1(8)	–	86.8± 6.1	86.8
Copolymers of PEGDM(13) and PEGDM(3)					
0	0	146 1(6)	–	98.1± 8.3	98.1
44	24	140 1(7)	–	121.3± 6.6	95.4
69	47	134 2(6)	–	135.2±2.1	92.7
86	70	143 2(8)	187 3(15)	156.2± 7.5	90.2
100	100	144 1(8)	–	86.8± 6.1	86.8
Copolymers of PEGDM(13) and PEGDM(4)					
0	0	122 4(9)	–	96.9± 4.1	96.9
38	22	138 1(6)	–	101.8± 8.7	94.7
60	40	145 2(8)	–	103.8± 6.6	92.8
69	50	147 2(10)	180 3(14)	109.3± 6.6	91.8
84	71	149 1(11)	183 2(16)	87.3±12.2	89.7
89	74	150 2(10)	190 4(13)	80.6±10.5	72.7
100	100	144 2(8)	–	86.8± 3.1	86.8

Scanning rate was 10°C min^{-1}

[a] The number in parentheses is the width at half height of the peak (in °C)

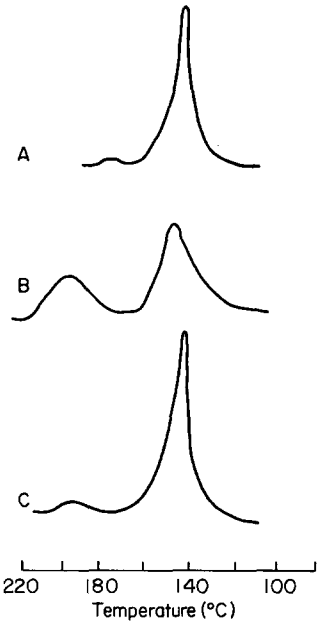

Figure 3 Representative d.s.c. polymerization exotherms of thermally scanned catalysed PEGDM(2)/PEGDM(13) comonomer mixtures in concentrations: (A) 27 mol% PEGDM(13); (B) 49 mol% PEGDM(13); (C) 72 mol% PEGDM(13)

the lack of initiator in the crosslink density regions leads to higher cure temperatures[27]. Such an inhomogeneous morphology has been observed by solid-state ^{13}C nuclear magnetic resonance (n.m.r.) and demonstrated graphically by a Monte Carlo computer simulation[12].

The absolute values of ΔH_{cure} of the neat, catalysed monomer in *Table 1* are close to those reported in the literature [105 kJ mol^{-1} for PEGDM(1) in ref. 24]. Joshi[25] also determined the energy of reaction of a single methacrylate moiety at 54.5 kJ mol^{-1} (dimethacrylates which are tetrafunctional would be expected to be approximately double this value).

The ΔH_{cure} (kJ mol^{-1}) for PEGDM(2), PEGDM(3), PEGDM(4) and PEGDM(13) are 115.2, 98.1, 96.9 and 86.8 kJ mol^{-1}, respectively. It is difficult to understand the decrease in ΔH_{cure} with increasing OE length. Whilst little similar d.s.c cure data were found in the literature for these systems, two main effects have been identified which would be expected to influence the exothermic energy evolved.

The first relates to the degree of residual unsaturation at full thermal cure. The short OE chains and tight networks formed by the three shortest OE length monomers usually mean that full cure is not possible and thus unsaturation remains, even at complete thermal cure due to inhomogeneous separation and entrapment of the active macroradical units from the remaining unsaturation within the network structure[12]. This would mean that the experimental ΔH_{cure} (in kJ mol^{-1} of reactive units) is lower than expected in the case in which all units were able to react. In the more flexible systems such as PEGDM(13) where entrapment of active species is not as likely, unsaturation at full thermal cure is not found[10]. According to this theory, however, shorter OE length monomers react incompletely, thus one would expect a lower ΔH_{cure}. *Table 1* indicates that, in fact, the opposite trend occurs.

Another possible effect on enthalpy of cure is also a function of OE length. It has been suggested[26] that in tightly crosslinked systems the physical stresses (bond stretching, rotation and bending) that occur in rigid vitrification of networks can absorb some of the liberated thermal energy, decreasing the amount eventually measured by d.s.c. The longer the OE chain, the less the expected energy loss by this mechanism. This is also contrary to the observed trend.

Therefore some other explanation must exist to explain the decrease in exotherm with increased OE length. A possibility is that the longer OE chains have stronger polar associations, entanglements and higher viscosities in the monomer state and during curing and that this provides some mechanism whereby exothermic energy is absorbed.

The position of the exotherm maxima, T_p, is scattered for different length monomers. Previous workers[27] have shown that T_p is a measure of reaction rate and depends inversely on initiator concentration. Such considerations are difficult in OEA systems since increasing the OE chain length increases flexibility and thus reaction rate whilst at the same time potentially increasing the viscosity of the system to a level where it may inhibit chain addition.

Differential scanning calorimetry scans of catalysed comonomers were measured over a range of compositions. The results for PEGDM(2)/PEGDM(13) and PEGDM(4)/PEGDM(13) are shown in *Figures 3* and *4*. PEGDM(3)/PEGDM(13) was also investigated, showed similar qualitative behaviour and is not graphically presented here. Tabulated results for all systems are presented in *Table 1*.

In many instances, two well-separated curing peaks were found to occur. The low temperature peak is labelled peak A and the high temperature peak as peak B. *Table 1* indicates that the peaks (when they occur) are well separated and the low temperature peak resides below that of the pure PEGDM(13) exotherm peak and that of the respective comonomer. Peak B exists at temperatures in excess of the curing exotherm of both comonomers and of the high temperature shoulder seen in some neat

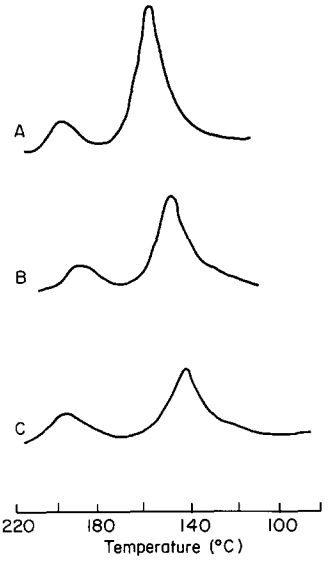

Figure 4 Representative d.s.c. polymerization exotherms of thermally scanned catalysed PEGDM(4)/PEGDM(13) comonomer mixtures in concentrations: (A) 50 mol% PEGDM(13(; (B) 71 mol% PEGDM(13); (C) 74 mol% PEGDM(13)

Table 2 Enthalpies of polymerization for peaks A and B in different copolymer systems where dual peaks are seen

Mol% PEGDM(13)	ΔH peak A (kJ mol^{-1})[a]	ΔH peak B (kJ mol^{-1})[a]
Copolymers of PEGDM(13) and PEGDM(2)		
27	127.3± 7.2(95)	6.3±3.1(5)
50	50.1± 4.5(35)	91.2±2.1(65)
72	130.1± 8.7(90)	9.5±4.3(10)
Copolymers of PEGDM(13) and PEGDM(3)		
70	147.0±10.8(94)	9.2±2.5(6)
Copolymers of PEGDM(13) and PEGDM(4)		
50	89.5± 8.9(82)	19.8±2.2(18)
69	65.5± 7.5(77)	21.8±3.4(23)
78	61.9±10.9(76)	18.7±8.1(24)

[a] The fraction (%) of each peak is given in parentheses

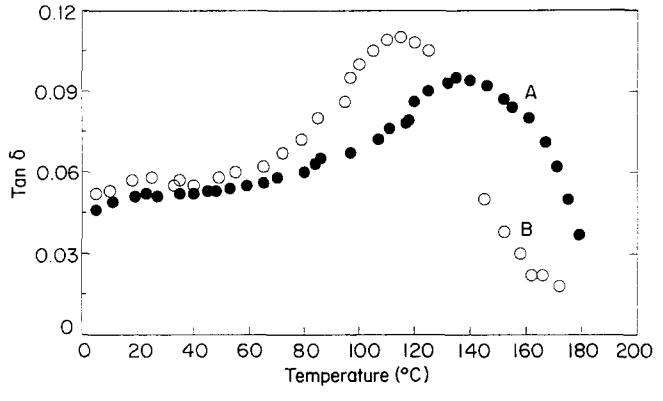

Figure 5 Dynamic mechanical loss tangent (tan δ)–temperature scans of (A) PEGDM(3) and (B) PEGDM(4) on a torsion pendulum

monomer systems, as described earlier. This clearly indicates that the system is copolymerizing in some complex, intermediate way and the two monomer phases are not grossly phase separating out and curing separately.

The ΔH_{cure} for the different copolymer systems show a consistent correlation between ΔH_{cure} and the copolymer concentration with the exotherm showing a maximum at intermediate PEGDM(13) concentrations. The PEGDM(13)/PEGDM(2) and PEGDM(13)/PEGDM(4) systems have a maximum value at about 50 mol% PEGDM(13) whilst in the PEGDM(13)/PEGDM(3) system this occurs at higher PEGDM(13) concentrations.

The reason for this behaviour is not clear. A simple, weighted law of mixtures calculation would yield exothermic values shown in *Table 1*. The increase in ΔH_{cure} with increasing amounts of PEGDM(13) at the low end of the concentration scale could be explained by systems becoming increasingly flexible. This would yield low degrees of residual unsaturation and greater energy output, as proposed earlier. The decrease in exotherm at higher PEGDM(13) concentrations is more difficult to understand but presumably the factors which cause the neat PEGDM(13) material to have the lowest ΔH_{cure} begin to dominate. The much higher value of the intermediate ΔH_{cure} (141.3 kJ mol^{-1} in the PEGDM(13)/PEGDM(2) system, for example) compared to the exotherms of the neat, constituent monomers is surprising. Clearly some complex, perhaps morphology-controlled, reaction results.

Table 2 indicates the relative sizes of peaks A and B to the overall exotherm for those comonomer blends which showed the double peak behaviour. It can be seen that there exists a wide range of relative sizes, both within a particular and between different blends. It is impossible at this stage to assign these peaks unequivocably given that there is no direct correlation between their relative size and PEGDM(13) concentration.

Dynamic mechanical tests were performed in the region of the glass transition on both homopolymers and copolymers, although at different concentrations than used in the d.s.c. studies. Since the aim of this work is essentially to discuss homogeneity of the copolymers by examining glass transition behaviour, lower temperature relaxations are presented elsewhere[17]. Since a large number of curves (of tan δ and G') were generated for the different copolymer series and for different concentrations within a particular series only the dynamic mechanical loss curves for PEGDM(3) and PEGDM(4) homopolymers (*Figure 5*), PEGDM(13) homopolymer (*Figure 6*) and the PEGDM(2)/ PEGDM(13) copolymer series (*Figure 7*) are reproduced here.

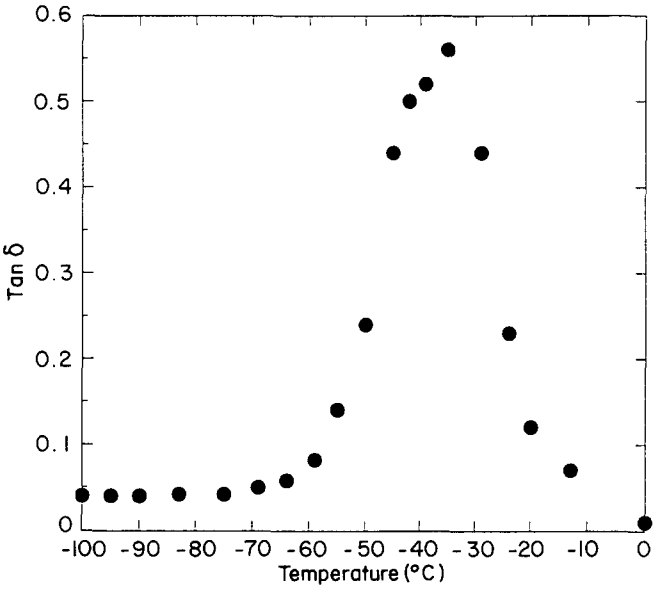

Figure 6 Dynamic mechanical loss tangent (tan δ)–temperature scan of PEGDM(13) on a torsion pendulum

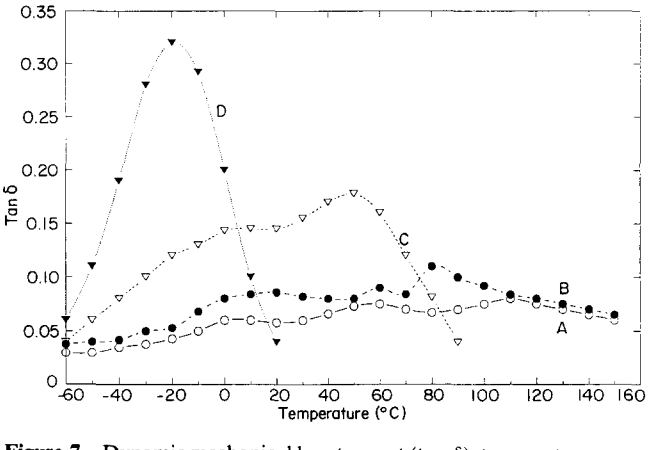

Figure 7 Dynamic mechanical loss tangent (tan δ)–temperature scans of PEGDM(2)/PEGDM(13) copolymers at PEGDM(13) mol% concentrations of: (A) 14%; (B) 23%; (C) 40%; (D) 76%

Table 3 Tabulated results of dynamic mechanical spectra of various copolymer systems

Mol% PEGDM(13)	T_g (°C)[a]	Width at half height of T_g peak	Log $G'(T_g+40°C)$ (G in N m^{-2})	Secondary peak (°C)[a]
Copolymers of PEGDM(13) and PEGDM(2)				
14	110(0.08)	190	8.27	55–60[b](0.08)
23	76(0.1)	168	8.05	63(0.08)
26	85(0.11)	160	8.03	60(0.11)
40	38(0.18)	100	7.65	–
76	−20(0.42)	35	7.21	–
100	−35(0.57)	24	6.99	–
Copolymers of PEGDM(13) and PEGDM(3)				
0	135(0.09)	180	8.30	–
25	73(0.15)	125	7.75	–
50	13(0.25)	70	7.41	–
75	−17(0.50)	33	7.15	–
100	−35(0.57)	24	6.99	–
Copolymers of PEGDM(13) and PEGDM(4)				
0	116(0.11)	110	8.10	–
21	52(0.20)	82	7.63	–
36	22(0.24)	64	7.45	–
64	−15(0.41)	40	7.18	–
75	−22(0.50)	27	7.14	–
100	−35(0.57)	28	6.99	–

[a] The value in parentheses is the peak height
[b] Broad shoulder

Relevant dynamic mechanical parameters for the glass transition region were abstracted from each curve for all copolymer systems and concentrations and are summarized in *Table 3*. A dynamic mechanical sample of pure PEGDM(2) homopolymer could not be made without it cracking due to high crosslink density (similar problems have been described elsewhere[29]) and thus the mechanical characteristics of this material could not be determined. It can be seen in the case of the homopolymers that PEGDM(13) is in the rubbery state at room temperature whilst PEGDM(2), PEGDM(3) and PEGDM(4) with their shorter OE chains and thus higher crosslink densities are glassy at ambient conditions.

It was found in a number of the PEGDM(2)/PEGDM(13) copolymers that double relaxations occurred in the region of T_g. In each instance the highest temperature peak was found to be greatest in height of the two relaxations and was assigned as the T_g. The double peak phenomena in the dynamic mechanical spectra of these systems will be discussed in more detail later.

Most of the copolymers showed a single glass transition which is indicative of monomer–monomer miscibility and random copolymerization. This is surprising given the inhomogeneous nature of the d.s.c. traces of catalysed OEA monomer and comonomer systems. The properties presented in *Table 3* decreased monotonically with increasing percentage mole fraction of the flexible PEGDM(13) monomer unit. The glass transition peak height monotonically increased in similar fashion. The variation of the properties is shown in *Figure 8* for copolymers of PEGDM(13) with PEGDM(2). A similar relationship between dynamic mechanical properties as a function of PEGDM(13) concentration was found in the other systems not shown graphically here. It was found that within a particular copolymer system a judicious scaling of the y-axis of the plot allows the parameters to exist on a common 'master' curve.

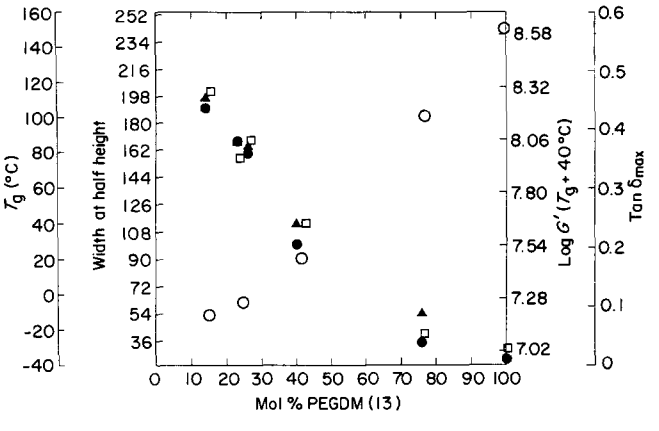

Figure 8 Variation of dynamic mechanical properties with mol% concentration of PEGDM(13) in a copolymer system with PEGDM(2). The properties shown are: (□) T_g; (○) tan δ_{max} (at T_g); (▲) log $G'(T_g+40°C)$; (●) width at half height

The downward trend in glass transition and rubbery modulus above T_g of copolymers of short OE chain monomers with increasing PEGDM(13) content is expected due to the lowering of the average crosslink density. Analogous behaviour is found in another system, that of copolymers between tetrafunctional OEA monomers and difunctional linear methacrylates such as methyl methacrylate[17,28]. In these systems, the linear methacrylate chains 'dilute' the crosslink density of PEGDM(4) and the decrease in rubbery modulus is

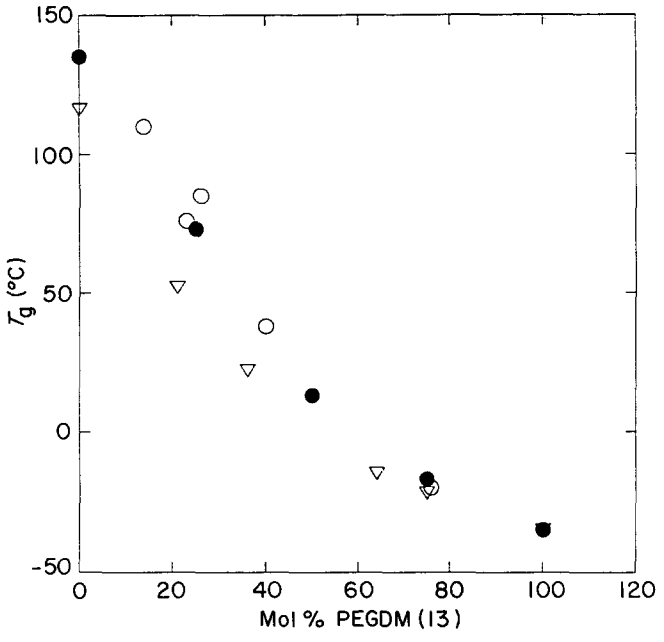

Figure 9 Glass transition temperature (highest temperature peak)–mol% PEGDM(13) for copolymer systems: (○) PEGDM(13)/PEGDM(2); (●) PEGDM(13)/PEGDM(3); (▽) PEGDM(13)/PEGDM(4)

found to obey the equation of state for a rubbery polymer[31]:

$$G = d \times R \times T/M_c \qquad (2)$$

where G = shear modulus, M_c = molecular weight between crosslinks, R = the gas constant, T = absolute temperature and d = density.

The glass transition behaviour for the three systems is plotted on a common PEGDM(13) concentration axis (*Figure 9*). The two shortest PEGDM(2) and PEGDM(3) copolymers behave similarly whilst that involving the more flexible PEGDM(4) shows slightly lower glass transitions. The graph can be extrapolated to obtain a T_g of 160°C for PEGDM(2) whose glass transition could not previously be determined due to brittleness of cured samples. The shape of the T_g *versus* percentage PEGDM(13) curve is similar to that found by Matsumato *et al.*[16] who copolymerized diallyl phthalate with various ethylene glycol bis(allyl phthalates). As with PEGDM(2) polymerization, they reported diallyl phthalate cracking on vitrification. However, copolymers produced with a high molecular weight monomer poly(ethylene glycol 600) bis(allyl phthalate) showed a similar decrease of T_g with decreasing crosslink density to that found here.

It is of interest to determine whether the variation of T_g with copolymer concentration can be modelled by the classical equation which describes the glass transition of linear copolymers based on the additivity of free volume of the two comonomers[32–34]. The equation is given below:

$$1/T_g = (1/w_1 + Bw_2)(w_1/T_{g_1} + Bw_2/T_{g_2}) \qquad (3)$$

where T_g = copolymer glass transition, T_{g_1} and T_{g_2} = the glass transitions of homopolymers 1 and 2, w_1 and w_2 = mass fractions of components 1 and 2, respectively, and B = a constant derived from the expansion coefficient of the samples in their glassy and rubbery states but is normally treated as an arbitrary parameter used to obtain the best fit. The equation is usually conveniently rearranged[34] into:

$$T_g = [k \times (T_{g_2} - T_g) \times w_2]/(1 - w_2) + T_{g_1} \qquad (4)$$

and plotted as T_g *versus* $[(T_{g_2} - T_g) \times w_2]/(1 - w_2)$. The T_{g_1} values of PEGDM(3) and PEGDM(4) are directly measurable. The extrapolated value of 160°C is used as T_{g_1} for PEGDM(2); T_{g_2} of PEGDM(13) is −35°C (*Table 3*).

The plot of equation (4) for each copolymer system is presented in *Figure 10*. A straight line fit as predicted by equation (4) was not seen to occur in any of the copolymer systems studied. It should be noted that equation (4) is based only on the copolymer effect—the additivity of free volume of different monomers. It does not take into account the network structure of a crosslinked polymer. It is perhaps surprising (and coincidental) that the copolymers of PEGDM(13) with PEGDM(2) and PEGDM(3) show such ideal behaviour given the complexities and inhomogeneities of the copolymerization reaction seen in the d.s.c. cure thermograms and dynamic mechanical behaviour.

Relatively few mathematical models have been proposed to predict the position of T_g relaxations in network copolymer systems specifically. Those that have assume that the copolymer and network effects are independent and additive. The model of Chompff[37], for example, treats the network as a series of chains, branch points and pendant ends. Many of the resultant parameters in the equation (effective volume of a chain end, dependence of T_g on chain end concentration and molecular weight) are difficult to calculate and only known for a few systems. These equations have been applied to copolymers between di- and tetrafunctional monomers, not to copolymers of two tetrafunctional systems, as studied here.

As mentioned earlier, many of the PEGDM(2)/PEGDM(13) copolymers were found to show two

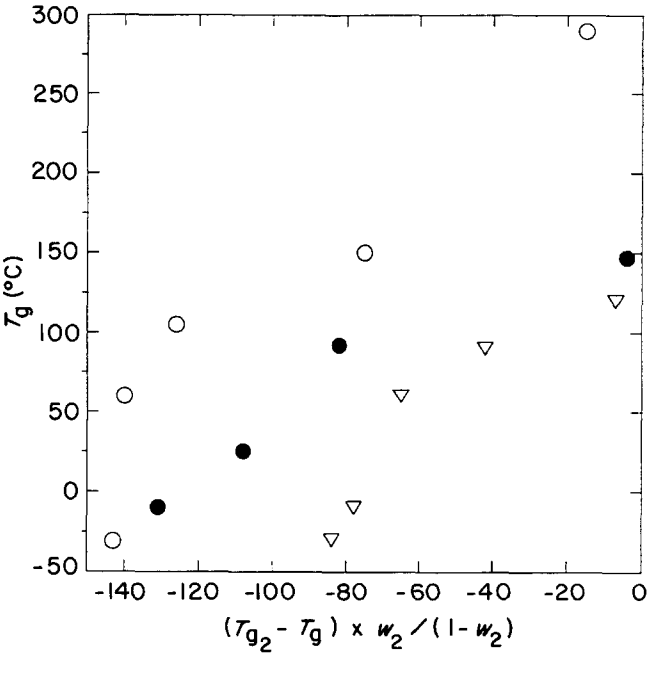

Figure 10 Plot of equation (4) for copolymer systems: (○) PEGDM(13)/PEGDM(2); (●) PEGDM(13)/PEGDM(3); (▽) PEGDM(13)/PEGDM(4)

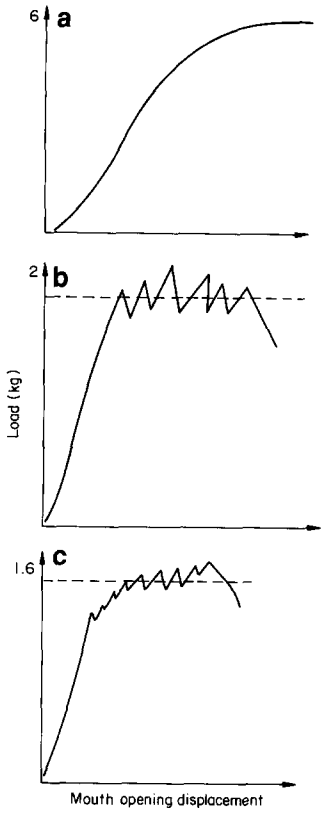

Figure 11 Representative mouth opening displacement–load traces for short rod fracture of: (a) PMMA; (b) PEGDM(4); (c) PEGDM(3) polymer

relaxations in the glass transition region (*Figure 8*). The position and heights of these are given in *Table 3*. The primary and secondary peaks are about the same height in each case. The secondary peak occurs at approximately the same position (55–63°C) in other copolymer compositions. This is much lower than the extrapolated T_g of 160°C for PEGDM(2) stated earlier and much higher than its subambient β relaxation (30°C) reported elsewhere[17]. This is further evidence that the two-phase behaviour is not simply pure PEGDM(2) material which has totally phase separated and cured independently. A similar effect was found by Bamford[38] in a copolymer of two linear systems [poly(methyl methacrylate), PMMA, and poly(vinyl trichloroacetate)] which showed dual peaks in the glass transition region, neither peak being the T_g of the homopolymers. This was ascribed to mixed microphases of the two systems. Complete phase separation and cure in dimethacrylate systems would be unlikely because the high functionalities of both components would inhibit gross monomer diffusion, even at low conversion. The fact that the glass transition relaxation peaks of PEGDM(3) and PEGDM(4) copolymers with PEGDM(13) do not show discrete, double peak phenomena could be explained by the fact that even if mixed microphase systems are formed, dynamic mechanical spectroscopy at ~1 Hz would not be able to resolve the glass transitions of different, small regions. It has been found in some polymer blend systems[39] that although optical microscopy can easily detect heterogeneity down to 0.01 μm, dynamical mechanical data yields only one peak, indicating a compatible system. Clearly compatibility is, by definition, related to the final domain size, the more finely dispersed a component, the more compatible it is claimed to be.

The other possibility is that some form of interpenetrating network is formed due to the differential rates of cure of the comonomers and the effects of high crosslink densities. The polymerization could be sequential [for example, PEGDM(13) cures initially, followed by PEGDM(3)]. The d.s.c. data summarized in *Table 1* support the concept of a complex polymerization process. The copolymerized system showed major peak positions of exotherms close to, but greater than, either pure system (peak A). The maximum temperature of peak B is greater again. Clearly some form of either copolymerization, interpenetration or partial phase separation may be occurring.

Short rod fracture was performed on a number of polymeric systems. To check the validity of the values of K_{IC} obtained by this method a sample of commercial, medium molecular weight PMMA was machined into the short rod geometry described earlier. When tested on the Instron it yielded the smooth, mouth opening displacement *versus* load curve shown in *Figure 11*. The level of the plateau yielded a K_{IC} of 0.94 ± 0.08 MN m$^{-3/2}$, a value well within the range 0.9–1.0 MN m$^{-3/2}$ quoted elsewhere[40]. Homopolymer samples of PEGDM(3) and PEGDM(4) were also cured and tested. The traces are also shown in *Figure 11*. As before, the tightly crosslinked nature of PEGDM(2) prevented the preparation of uncracked samples. The K_{IC} values for the glassy systems yielded values of 0.12 ± 0.03 MN m$^{-3/2}$ [PEGDM(3)] and 0.2 ± 0.04 MN m$^{-3/2}$ [PEGDM(4)]. Samples of PEGDM(13) were rubbery and are, by definition, inappropriate for use in this technique designed essentially for glassy systems. Their failure mechanism is more related to tearing than crack growth. However, for comparison later with the copolymers a value of 0.016 ± 0.002 MN m$^{-3/2}$ was obtained for PEGDM(13).

The value of K_{IC} can be related by the following expression to γ_p (J m^{-2}), the energy required to form new surfaces where there is plastic flow[41]. Plastic flow is a modification of linear fracture mechanics where the energy to form a new polymer surface (γ) is related mainly to polymer bond cleavage. The relevant equation of Andrews[42] is:

$$K_{IC}^2/2E = \gamma_p \qquad (5)$$

where Young's modulus, E, at room temperature has been determined elsewhere[17]. The resulting values of γ_p for the dimethacrylate OEA series are 14 J m^{-2} [PEGDM(3)] and 27 J m^{-2} [PEGDM(4)]. Two other fracture techniques (Charpy impact and instrumented impact testing[17]) also confirmed the greater fracture toughness of PEGDM(4) over the more highly crosslinked PEGDM(3).

Both the mouth opening displacement shape and the level of the load of the crosslinked OEA system differed from that of the PMMA sample. Whereas PMMA showed a smooth curve, both the PEGDM(3) and PEGDM(4) curves displayed saw-tooth traces. This is typical of the stick-slip mechanism seen in many brittle, thermosetting polymers during fracture testing. Fracture techniques such as double torsion fracture also show saw-toothed load *versus* displacement curves in crosslinked systems[40]. This is usually known as the 'stick-slip' fracture mode and arises from a series of crack initiations and arrests. This phenomenon can be seen by comparing photomicrographs of the fracture surfaces of PMMA

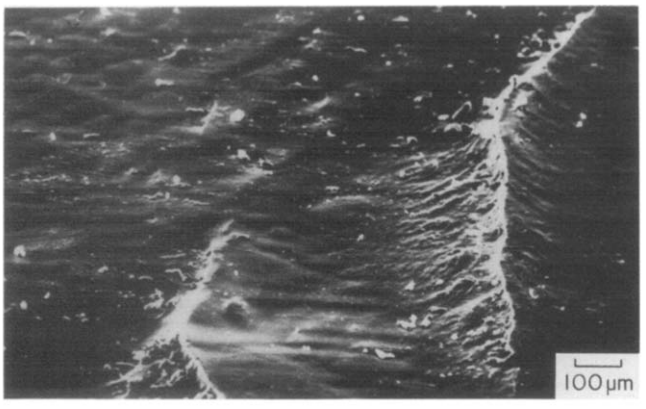

Figure 12 Scanning electron micrograph of short rod fracture surface of PMMA

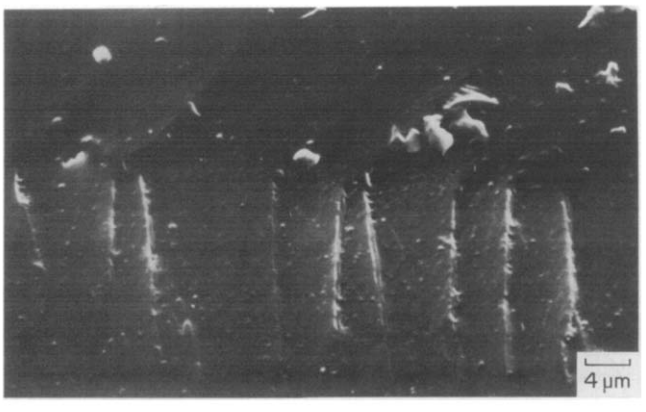

Figure 13 Scanning electron micrograph of short rod fracture surface of PEGDM(4)

(*Figure 12*) and PEGDM(4) (*Figure 13*). The PMMA surface shows ridges representative of gross plastic flow whilst that of PEGDM(4) is smooth with lines of arrest and initiation clearly seen.

It is surprising that the short rod and other fracture techniques[17] were able to differentiate between the two glassy polymers, PEGDM(3) and PEGDM(4), at room temperature since short range forces are thought to dominate in the fracture of these materials rather than longer range relaxational motions[43] that arise from copolymers with different OE lengths. However, the difference in fracture toughness can be explained with reference to OE length, but due to morphological rather than relaxational considerations.

It is proposed that fracture in such brittle systems occurs by cracks propagating via points of lowest strength. Golikov[44] suggests that in glassy dimethacrylates this is related to the inhomogeneous nature of the system with the weakest regions being the less highly crosslinked, lower density material situated between high density polymer clusters. Such a model has also been proposed in epoxies[45–47] where a nodular morphology is often assumed. As mentioned earlier, it has been shown[10] by solid-state ^{13}C n.m.r. that the unsaturation in PEGDM(3) is 12% whilst in PEGDM(4) it is 2%. It has been demonstrated by computer simulation that in tetrafunctional systems the residual unsaturation (monomer and pendant double bonds) exists in between nodules of highly crosslinked material[12,47]. Thus PEGDM(3) would be more inhomogeneous, have more points of weakness and thus a lower fracture energy would be expected. This model of fracture toughness is also of importance when considering the copolymers' fracture toughness.

Fracture toughness measurements were carried out on copolymers of PEGDM(13) and PEGDM(4) with varying copolymer compositions. The results seen in *Table 4* show that there is a monotonic increase in fracture toughness with increasing PEGDM(4) content. The increase is most noticeable in the sample with 21.3 mol% PEGDM(13)/78.7 mol% PEGDM(4) which is a glassy polymer with a T_g of 50°C. Further increases in the glassy material [higher PEGDM(4) content] result in still greater fracture toughness. This is opposite to results of Matsumato and Oiwa[16] who found that increasing the flexible chain content in the copolymerization of two tetrafunctional monomers (and thus decreasing average crosslink density) increased the fracture toughness.

Previous work in fracture toughness of crosslinked copolymers has been done with copolymers of bifunctional monomers. Martin[49] found that by increasing the crosslinking monomer component, fracture toughness decreased and the fracture surface changed from crazing to the smooth surface associated with brittle fracture. Conversely (and similar to the results presented here) Gomes and Timbo[48] found that copolymerizing methyl methacrylate and PEGDM(3) resulted in greater fracture toughness with higher PEGDM(3) content. They explained this by assuming that significant cyclization of PEGDM(3) units occurred and that these pendant groups absorbed the fracture energy. Such an assertion is difficult to verify in immiscible, crosslinked systems.

Figure 14 shows the load *versus* displacement curves for the copolymers tested in this work. As the PEGDM(13) content increases, the peak load value decreases and the curves indicate less of a 'stick-slip' mechanism but failure more akin to fracture of a thermoplastic (i.e. PMMA). However, unlike linear polymers which have high fracture toughness, the value of K_{IC} decreases with increasing flexible PEGDM(13) content. An explanation for this behaviour is that, in addition to regions of low crosslink density found in a heterogeneous dimethacrylate homopolymer, there exist regions in the copolymer in which higher proportions of PEGDM(13) reside. These regions will be of very low crosslink density and it is through these regions of weakness that the crack propagates.

CONCLUSIONS

Thermal scans of pure catalysed dimethacrylate monomer indicate a heterogeneous curing process. This arises due to the highly branched structures that form at very low

Table 4 Stress intensity factor (K_{IC}) determined by the short rod fracture method for the PEGDM(13)/PEGDM(4) copolymer system at 25°C

Mol% PEGDM(13)	T_g (°C)	K_{IC} (MN m$^{-3/2}$)
0.0	115	0.275±0.043
9.8	98	0.269±0.023
21.3	52	0.258±0.032
27.5	40	0.0622[a]
33.6	32	0.024±0.012
100.0	−5	0.016±0.002

[a] Only one sample tested

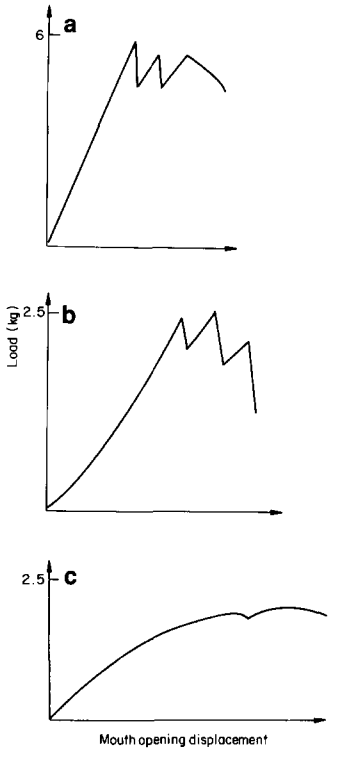

Figure 14 Representative mouth opening displacement–load traces for short rod fracture of PEGDM(13)/PEGDM(4) copolymers with PEGDM(13) mol% concentration of: (a) 0%; (b) 9.8%; (c) 21.3%

levels of cure in these systems. Differential scanning calorimetry and dynamic mechanical spectroscopy indicate that further complexity of cure is introduced when one investigates the copolymerization of dimethacrylate monomers of different OE length. The resultant inhomogeneity is illustrated by two separate peaks (peaks A and B) in the d.s.c. curing exotherms in all the copolymer systems investigated. The positions of the two d.s.c. curing peaks in the copolymer systems are at different temperatures than either of the constituent catalysed monomers.

Two-peak behaviour in the glass transition region is also seen in the PEGDM(13)/PEGDM(2) system of the dynamic mechanical spectra. Despite this inhomogeneity of properties, many of the other dynamic mechanical variables of the copolymers show a smooth gradation between those of the constituent homopolymer systems. This monotonic property variation with copolymer composition expected in simple copolymer systems, indicates that some copolymerization must also occur, in addition to some partial phase separation. The nature of this partial phase separation is not able to be fully characterized at this stage. The fact that double glass transition peaks were not seen in all copolymer systems may be due to the limited resolution such a dynamic mechanical technique has for determining the compatibility of phases.

Fracture behaviour in these highly crosslinked systems is interpreted in terms of failure via points of weakest strength. In the homopolymer this is most likely to be the less crosslinked regions existing between the heterogeneous nodules of highly crosslinked material ('porridge model'). These weak, interstitial regions are thought to consist mainly of pendant double bonds and residual monomer[12]. The fact that the fracture toughness of the copolymer blends decreases monotonically with the addition of more flexible PEGDM(13) material (lower K_{IC}) and the failure mode transforms from the brittle, stick-slip fracture mode to smoother crack propagation (as shown by mouth opening displacement *versus* load curves) indicates that failure in the copolymer systems may also be via points of weakness, possibly through interstitial regions of high PEGDM(13) concentration.

REFERENCES

1 Bowman, C. N., Carver, A. L., Kennett, S. N., Williams, M. and Peppas, N. A. *Polymer* 1990, **31**, 135
2 Kloosterboer, J. G. *Adv. Polym. Sci.* 1989, **84**, 1
3 Ryter, I. E. and Oyased, H. J. *J. Biomed. Mater. Res.* 1987, **21**, 11
4 Craig, R. G. (ed.) 'Restorative Dental Materials', 6th Edn., C.V. Mosby Company, St Louis, 1980
5 Kloosterboer, J. G. and Lippits, G. J. M. *J. Rad. Cur.* 1984, **11**(1), 10
6 Blyer, L. L., DiMarcello, F.V., Hart, A. C. and Huff, R. G. *Polym. Mater. Sci. Eng.* 1986, **55**, 536
7 Zweiers, R. J. M. and Dorant, G. C. M. *Appl. Opt.* 1983, **22**, 2410
8 American Dental Society Council on Dental Materials *JADA* 1986, **112**, 707
9 Roulet, J. F. 'Degradation of Dental Polymers', Karger, Basel, 1987
10 Allen, P. E. M., Simon, G. P., Williams, D. R. G. and Williams, E. H. *Macromolecules* 1989, **22**, 809
11 Korolev, G. V., Smirnov, B. R., Zhil'tsova, L. A., Makhonina, L. I., Tvogorov, N. V. and Berlin, A. A. *Vysokmol. Soedin Ser. A* 1967, **19**, 9
12 Simon, G. P., Allen, P. E. M., Bennett, D., Williams, D. R. G. and Williams, E. H. *Macromolecules* 1989, **22**, 3555
13 Malinsky, J., Klaban, J. and Dusek, K. *J. Macromol. Sci.* 1971, **A5**, 1071
14 Boots, H. J. and Dotson, N. A. *Polym. Commun.* 1988, **29**, 346
15 Suzuki, Y., Fujimoto, T., Tsunoda, S. and Shibayama, K. *J. Macromol. Sci.* 1980, **B17**(4), 7987
16 Matsumato, A. and Oiwa, M. *Polym. Prepr.* 1984, **25**(1), 138
17 Simon, G. P. *PhD Thesis* University of Adelaide, 1987
18 Cowperthwaite, G. F., Foy, J. J. and Malloy, M. A. 'Biomedical and Dental Applications of Polymers' (Eds C. G. Geblen and F. Koblitz), Plenum Press, New York, 1981
19 Barker, L. M. *Eng. Fract. Mech.* 1977, **9**, 361
20 Barker, L. M. *Int. J. Fract.* 1979, **15**(6), 515
21 McClintock, F. A. and Irwin, G. R. 'Fracture Toughness and Testing and its Applications', ASTM STP 381, 1965
22 Koblitz, F. F., Luna, V. R., Glenn, J. F. and DeVries, K. L. *Polym. Eng. Sci.* 1979, **19**(9), 607
23 Barker, L. M. 'Short Bar Specimens for K_{IC} Measurements', ASTM STP 678, 1981
24 Moore, J. in 'Chemistry and Properties of Crosslinked Polymers' (Ed. S. S. Labana), Academic Press, New York, 1977
25 Joshi, R. M. *J. Polym. Sci.* 1962, **56**, 313
26 Ozerkovskii, B. V. and Roschupkin, V. P. *Doklady. Akademii Nauk SSSR* 1979, **248**(3), 657
27 Kenyon, L. and Nielsen, L. C. *J. Macromol. Sci.* 1969, **A3**(2), 275
28 Horie, K., Otagawa, A., Muraoka, M. and Mita, I. *J. Polym. Sci., Polym. Chem. Edn.* 1975, **13**, 445
29 Loshaek, S. and Fox, T. G. *J. Am. Chem. Soc.* 1953, **75**, 3544
30 Loshaek, S. and Fox, T. G. *J. Polym. Sci.* 1955, **15**, 371
31 Nielsen, L. E. *Rev. Makromol. Chem.* 1970, **4**, 69
32 Mandelkern, L., Martin, G. F. and Quinn, F. A. *J. Res. Natl. Bur. Std.* 1957, **58**(3), 137
33 Pochan, J. M. and Beatty, C. L. *Polymer* 1979, **20**, 879
34 Wood, L. A. *J. Polym. Sci.* 1958, **28**, 319
35 Martin, G. C., Mehta, R. K. and Lott, S. E. *Polym. Prepr.* 1989, **22**(2), 319
36 Dimarzio, E. *J. Res. Natl. Bur. Std.* 1984, **68A**, 611
37 Chompff, A. J. in 'Polymer Networks' (Eds A. J. Chompff and S. Newman), Plenum Press, New York, 1971
38 Bamford, C. H., Eastmond, G. C. and Whittle, D. *Polymer* 1975, **16**, 377
39 Matsuo, M., Nozaki, C. and Jyo, Y. *Polym. Eng. Sci.* 1969, **9**(3), 197
40 Young, J. and Beaumont, P. W. *J. Mater. Sci. Lett.* 1976, **11**, 776

41 Irwin, G. R. *J. Appl. Mech.* 1957, **24**, 361
42 Andrews, E. H. 'Fracture in Polymers', Oliver and Boyd, Edinburgh, 1968
43 Lemay, J. B., Sveltin, B. J. and Kelly, F. N. *ACS Symp. Ser.* 1984, **243**
44 Golikov, I. V., Berezin, M. P., Mogilevich, M. M. and Korolev, G. *Vsokmol. Soedin.* 1979, **A21**, 1824
45 Labana, S. S., Newman, S. and Chompff, A. J. 'Polymer Networks' (Eds A. J. Chompff and S. S. Newman), Plenum Press, New York, 1971
46 Mojovic, J. and Koutsky, J. A. *Polymer* 1979, **20**, 1095
47 Boots, H. M. J. and Pandey, R. B. *Polym. Bull. (Berlin)* 1984, **11**, 415
48 Gomes, A. S. and Timbo, A. M. *Polym. Eng. Sci.* 1981, **21**(12), 745
49 Martin, G. C., Mehta, R. K. and Lott, S. F. *Polym. Prepr.* 1981, **22**(2), 319